Eur. Phys. J. C (2019) 79:848
https://doi.org/10.1140/epjc/s10052-019-7343-x

THE EUROPEAN PHYSICAL JOURNAL C

Regular Article - Theoretical Physics

Exploring the deviation of cosmological constant by a generalized pressure parameterization

Jun-Chao Wang[1,2,a], **Xin-He Meng**[1,b]

[1] Department of Physics, Nankai University, Tianjin 300071, China
[2] Jinshan School of Longyan Number One High School, Longyan 364000, China

Received: 21 July 2019 / Accepted: 23 September 2019 / Published online: 15 October 2019

Abstract We bring forward a generalized pressure (GP) parameterization for dark energy to explore the evolution of the universe. This parametric model has covered three common pressure parameterization types and can be reconstructed as quintessence and phantom scalar fields, respectively. We adopt the cosmic chronometer (CC) datasets to constrain the parameters. The results show that the inferred late-universe parameters of the GP parameterization are (within 1σ): the present value of Hubble constant $H_0 = (72.30^{+1.26}_{-1.37})$ km s^{-1} Mpc^{-1}; the matter density parameter $\Omega_{m0} = 0.302^{+0.046}_{-0.047}$, and the bias of the universe towards quintessence. Then we perform a dynamic analysis on the GP parameterization and find that there is an attractor or a saddle point in the system corresponding to the different values of the parameters. Finally, we discuss the ultimate fate of the universe under the phantom scenario in the GP parameterization. It is demonstrated that the three cases of pseudo rip, little rip, and big rip are all possible.

1 Introduction

Over the past two decades, a large number of cosmological observations have confirmed that the expansion of the late universe is speeding up [1–5], which has become one of the greatest challenges of cosmology. In order to explain the accelerated expansion, there are two main approaches: modifying gravity (MG) and adding dark energy (DE). The former means modifying the geometric parts of general relativity (GR), such as scalar-tensor theory [6], $f(R)$ gravity [7,8] and brane cosmology [9,10]. The other method is to add the dark energy, which breaks the strong energy condition and produces a mysterious repulsive force to make the universe accelerate the expansion. The simplest DE model is the ΛCDM model, where the cosmological constant Λ is related to DE, and its equation of state (EoS) is $\omega_{de} = -1$. The ΛCDM model provides a fairly good explanation for current cosmic observations. Recently, Planck-2018 reaffirmed the validity of the six-parameter ΛCDM model in describing the evolution of the universe [11]. Nonetheless, there are two long-term problems with the ΛCDM model. One is the fine-tuning problem: The observation of dark energy density is 120 orders of magnitude smaller than the theoretical value in quantum field theory [12,13]; the second is the coincidence problem: At the beginning of the universe, the proportion of DE is especially tiny while now the dark energy density and matter density are exactly of the same magnitude. Besides, in recent years, the tension of Hubble constant between the Planck datasets and SHoES has reached 4.4σ [14], which are brought about by the ΛCDM model and the cosmic distance ladder method, respectively. So as to alleviate these problems, many dynamic dark energy models with the time-variation EoS are proposed, including scalar field models (such as quintessence [15–19], phantom [20–22], k-essence [23–25], quintom [26–28] and tachyon [29]), holographic model [30], agegraphic model [31], Chaplygin gas model [32,33].

The model presented in this paper is also a dynamic dark energy model, which parameterizes the total pressure of the universe. Parameterization of the observable is an effective method to explore the characteristics of DE, such as the parameterization of EoS [34–36], the luminosity distance [37,38], dark energy density [39], pressure [40–45] and deceleration factors [46]. Take the pressure parameterization as an example. In general, we can write the pressure parameter equation as $P = \sum_{n=0} P_n x_n(z)$, where $x_n(z)$ expands for the late universe in the following forms: (i) redshift: $x_n = z^n$, (ii) scale factor: $x_n(z) = (1-a)^n = (z/(1+z))^n$, (iii) logarithmic form: $x_n(z) = (\ln(1+z))^n$. The form corresponding to $n = 1$ in (i) and (ii) was proposed by Zhang et al. [42]. Case (iii) for $n = 1$ was given by Wang

[a] e-mail: dakaijun@dakaijun.cn
[b] e-mail: xhm@nankai.edu.cn

and Meng [45]. In order to unify these mainstream parameterization methods, we suggest a three-parameter pressure parameterization model to explore the evolution of the universe.

This paper is organized as follows: Sect. 2 presents a generalized pressure (GP) parameterization of the total pressure and discusses its feature. In Sect. 3, we use CC datasets to impose constraints on the parameters of the GP parameterization. The discussion of fixed points using the GP parameterization is analyzed in Sect. 4. In Sect. 5, we exhibit the end of the universe under the phantom case. Section 6 is for the conclusion.

2 Theoretical model

Pressure parameterization describes our universe in the following ways: First, hypothesize a relationship between the pressure P and the redshift z. Then the expression of the density ρ can be derived from the conservation equation $\dot{\rho}+3(\dot{a}/a)(\rho+P)=0$. Finally, by utilizing the Friedmann equations $H^2=3/(8\pi G)\sum_i \rho_i$ and the EoS $\omega=P/\rho$, we can get the form of the Hubble parameter H and ω, respectively. Here we take the speed of light $c=1$. At this point, a closed system of cosmic evolution has been established which is described by the Friedmann equations, the conservation equation, and the EoS form.

It is worth noting that there are still some deviations between the ΛCDM and actual data (e.g., H_0 tension), but the physical mechanism behind it is not clear. Taking advantage of this kind of ad hoc model, we can probe the possible deviations further between the dynamic case and the cosmological constant case without a specific premise. In this work, we propose a generalized pressure parameterization of the total energy components in a spatially flat Fridenmann–Robertson–Walker (FRW) universe:

$$P(z)=P_1-P_2\left[\frac{(1+z)^{-\beta}-1}{\beta}\right],\quad \beta\neq 0, \tag{1}$$

where P_1, P_2 and β are free parameters. Notice that P_1 is the current value of the total pressure in the universe, and P_2 represents the deviation of $P(z)-z$. The model degenerates into the ΛCDM model as $P_2=0$. We point out that this parametric form of $P(z)$, i.e. Eq. (1), is inspired by a generalized equation of state for dark energy [36]. When specific limits are given to β, this model returns to the three models mentioned in Sect. 1, i.e.,

$$P(z)=\begin{cases} P_a+P_b z, & \text{for } \beta=-1,\\ P_a+P_b\ln(1+z), & \text{for } \beta\to 0\\ P_a+P_b\left(\frac{z}{1+z}\right), & \text{for } \beta=+1. \end{cases} \tag{2}$$

By using Eq. (1), the relationship of the scale factor a ($a=1/(1+z)$) and the conservation equation ($\dot{\rho}+3(\dot{a}/a)(\rho+P)=0$), we can get the density:

$$\rho(a)=\frac{3a^{\beta}P_2}{(3+\beta)\beta}-\frac{P_2}{\beta}-P_1+Ca^{-3}, \tag{3}$$

where C is the integral constant. We assume ρ_0 is the current total density, i.e. $\rho(a=1)=\rho_0$. Finally, the total density and total pressure can, respectively, be written in the following form:

$$\rho(a)=\rho_0(P_a a^{\beta}+\Omega_{\mathrm{m0}}a^{-3}+1-P_a-\Omega_{\mathrm{m0}}), \tag{4}$$

$$P(a)=\rho_0\left[-(1-P_a-\Omega_{\mathrm{m0}})-\frac{3+\beta}{3}P_a a^{\beta}\right]. \tag{5}$$

The parameters P_1 and P_2 have been replaced here by the new parameters P_a and Ω_{m0}, where $P_a\equiv 3P_2/((3+\beta)\beta\rho_0)$, $\Omega_{\mathrm{m0}}\equiv(\beta\rho_0+P_2+\beta P_1-3P_2/(3+\beta))/(\beta\rho_0)$. In the density expression (4), the item $\rho_0\Omega_{\mathrm{m0}}a^{-3}$ corresponds to the matter density ρ_m. So $\Omega_m|_{a=1}=\rho_m/\rho=\Omega_{\mathrm{m0}}$ signifies the physical meaning of the parameter Ω_{m0}; it is the present-day matter density parameter. The term $\rho_0(P_a a^{\beta}+1-P_a-\Omega_{\mathrm{m0}})$ accords with the dark energy density ρ_{de}, and the constant part $1-P_a-\Omega_{\mathrm{m0}}$ looks similar to the ΛCDM case. The term $P_a a^{\beta}$ makes ρ_{de} change with time: The larger $|P_a|$ is, the higher the deviation from the ΛCDM model will be; the larger β is, the faster the dark energy density will change. Accordingly, this cosmological model only includes matter and dark energy components, and the pressure of the dark energy P_{de} is the total pressure P. Note that when $\beta=-3$, the density of the part of the dark energy is expressed as the matter density, and the total density $\rho(a)$ of our GP parameterization has the same form as the ΛCDM model.

Suppose the dark energy is a scalar field ϕ that changes with time. The corresponding pressure and density are equivalent to $\rho_{\mathrm{de}}=(n/2)\dot{\phi}^2+V(\phi)$ and $P_{\mathrm{de}}=(n/2)\dot{\phi}^2-V(\phi)$, separately, where $n=1$ or -1 corresponds to the quintessence and phantom scalar field, respectively. The calculation shows that $\dot{\phi}^2=-(n\beta/3)\rho_0 P_a a^{\beta}$, so $\beta P_a<0$ fits quintessence, and $\beta P_a>0$ matches the phantom model.

Additionally, for the GP parameterization, the EoS of the dark energy ω_{de}, the dimensionless Hubble parameter E, the deceleration parameter q and the jerk parameter j, respectively, take the form

$$\omega_{\mathrm{de}}=-1-\frac{\frac{1}{3}\beta P_a a^{\beta}}{1-P_a-\Omega_{\mathrm{m0}}+P_a a^{\beta}}, \tag{6}$$

$$E=(\Omega_{\mathrm{m0}}a^{-3}+P_a a^{\beta}+1-P_a-\Omega_{\mathrm{m0}})^{1/2}, \tag{7}$$

$$q\equiv-\frac{\ddot{a}}{aH^2}=-1+\frac{3}{2}\Omega_m-\frac{\beta P_a}{2E^2}a^{\beta}, \tag{8}$$

$$j\equiv\frac{\dddot{a}}{aH^3}=1+2(q+1)(2q-1)-\frac{a^{\beta}P_a\beta((\beta+3)}{2E^2}. \tag{9}$$

Table 1 Cosmic chronometers data used in this paper

z	$H(z)$	$\sigma_{H(z)}$	References	z	$H(z)$	$\sigma_{H(z)}$	References	z	$H(z)$	$\sigma_{H(z)}$	References
0.07	69	19.68	[47]	0.36	81.2	5.9	[48]	0.7812	105	12	[48]
0.09	69	12	[49]	0.3802	83	13.5	[50]	0.8754	125	17	[48]
0.1	69	12	[51]	0.4	95	17	[52]	0.88	90	40	[51]
0.12	68.6	26.2	[47]	0.4004	77	10.2	[50]	0.9	117	23	[52]
0.17	83	8	[52]	0.4247	87.1	11.2	[50]	1.037	154	20	[48]
0.1791	75	4	[48]	0.4497	92.8	12.9	[50]	1.3	168	17	[52]
0.1993	75	5	[48]	0.47	89	50	[53]	1.363	160	33.6	[54]
0.2	72.9	29.6	[47]	0.4783	80.9	9	[50]	1.43	177	18	[52]
0.27	77	14	[52]	0.48	97	62	[51]	1.53	140	14	[52]
0.28	88.8	36.6	[47]	0.5929	104	13	[48]	1.75	202	40	[52]
0.3519	83.0	14	[48]	0.6769	92	8	[48]	1.965	186.5	50.4	[54]

Table 2 The priors and initial seeds of parameters used in the posterior analysis

Parameter	Prior	Initial seed
H_0	[0, 100]	69
Ω_{m0}	[0, 1]	0.33
P_a	[− 1, 1]	0
β	[− 5, 5]	− 0.02

3 Results of the data analysis

By measuring the age difference between two galaxies under different redshifts, we can get the Hubble constant $H(z)$, called cosmic chronometer data. In this section, we constrain our parameter by the 33 unrelated cosmic chronometer data listed in Table 1, spanning the redshift range $0 < z < 2$. The optimal values of the parameters can be obtained by taking the minimum value of χ^2, which is expressed as

$$\chi^2 = \sum_{i=1}^{33} \left[\frac{H_{\rm obs}(z_i) - H_0 E(z_i)}{\sigma_i^2} \right]^2, \tag{10}$$

with the corresponding four-dimensional parameter space $\{H_0, \Omega_{m0}, P_a, \beta\}$.

We adopt the Monte Carlo Markov chain (MCMC) method and use the python package emcee [55] to produce a MCMC sample with CC data. The results are displayed as a contour map by another python package, pygtc [56]. We list the priors and initial seeds on the parameter space in Table 2. Figure 1 shows the one-dimensional and two-dimensional marginalized probability distributions of the GP parameterization. In the meantime, the best-fit values and 1σ confidence level for the H_0, Ω_{m0}, P_a and β are listed in Table 3. From the constraint results, $P_a\beta < 0$ in 1σ, which indicates that our universe is in a quintessence situation and has some deviation from the ΛCDM model from the point of view of the data. The differences of H_0 between our results and SHoES [14] and the Planck base-ΛCDM [11] are 0.9 σ and 3.5 σ, respectively. This suggests that the GP parameterization is more supportive of the results of SHoES. The ΛCDM model is not the best form in this general framework and shows some difference from the best form.

The evolution of the DE EoS parameter ω_{de}, the DE density parameter Ω_{de}, the deceleration parameter q and the jerk parameter j with 1σ error propagation from data fitting (Table 3) are shown in Fig. 2. From Fig. 2 we find that these results are acceptable, except for the DE density parameter Ω_{de}, which is too high at the beginning of the universe and contradicts the facts we now know. This parameterization is an approximation of the late universe, and the result of the DE density parameter suggests that it does not apply to the early universe. In addition, from $(\rho_{de}/\rho_m)|_{a\to 0,\beta>-3} \to 0$ we can see that, for the case of $\beta > -3$, the DE accounts for a small percentage in the early universe and the previous problem is avoided.

4 Dynamic analysis

In this section, we will construct a self-consistent dynamical system to analyze the cosmological evolution of the GP parameterization. Let us select Ω_{de} and E as independent variables. By Friedmann equation, we can get the self-consistent dynamic system

$$\Omega'_{de} = (1 - \Omega_{de}) \left(\beta\Omega_{de} - \frac{P_b\beta}{E^2} + 3\Omega_{de} \right), \tag{11}$$

$$E' = \frac{E}{2} \left[\beta\Omega_{de} - \frac{P_b\beta}{E^2} - 3(1 - \Omega_{de}) \right], \tag{12}$$

where $P_b \equiv 1 - P_a - \Omega_{m0}$, "$'$" represents the derivative of $\ln(a)$. The following are common methods for finding fixed points and its stability of a system. Let $\Omega'_{de} = E' = 0$, then,

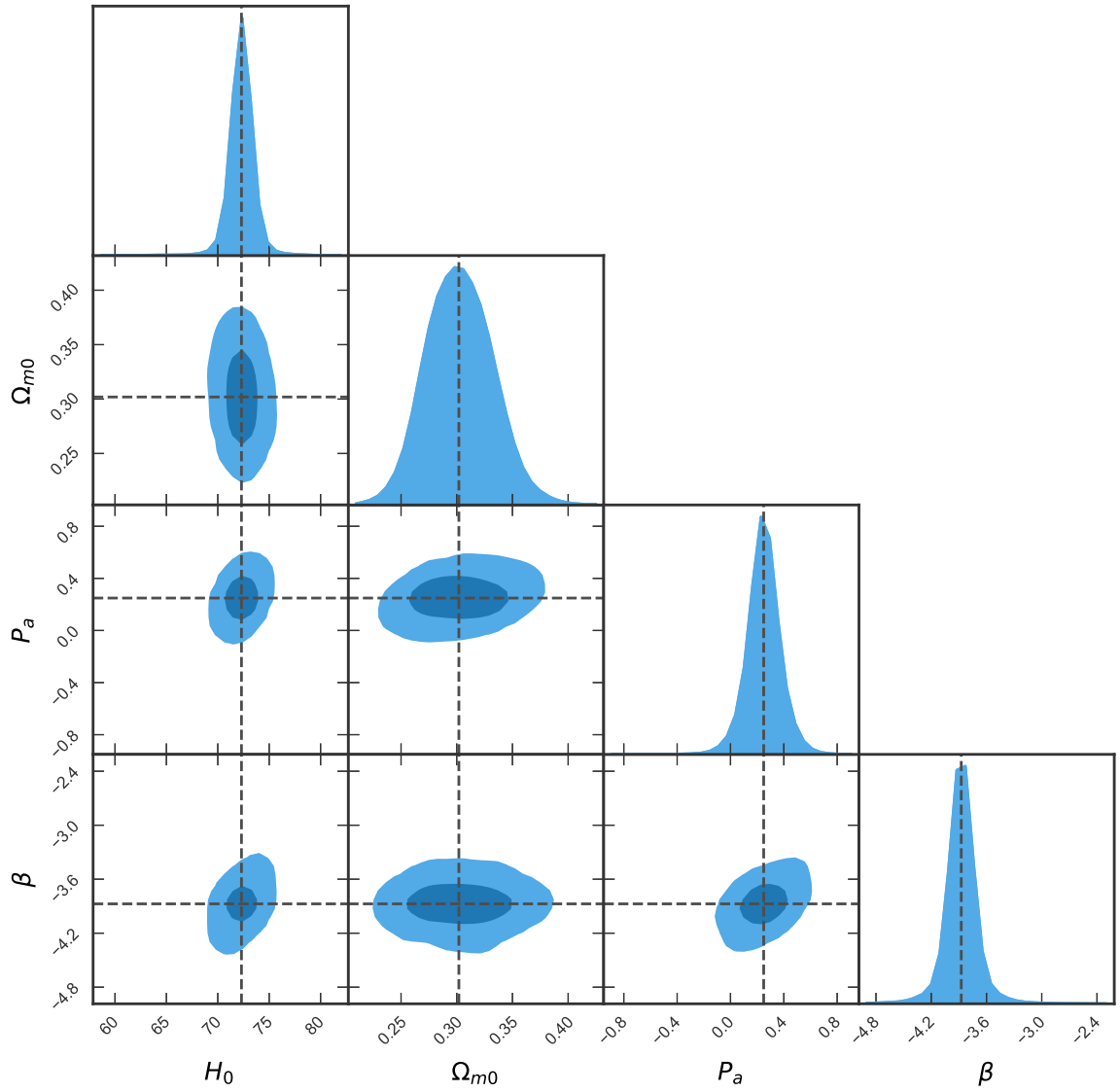

Fig. 1 The one-dimensional and two-dimensional marginalized probability distributions of the GP parameterization by using CC observations. The dark blue and light blue areas represent 1σ and 2σ errors, respectively

Table 3 Best-fit parameters H_0, $\Omega_{\rm m0}$, P_a and β from CC datasets. Here we also list χ^2_{min}

Parameter	Best-fit value with 1σ error
H_0	$72.30^{+1.26}_{-1.37}$
$\Omega_{\rm m0}$	$0.302^{+0.046}_{-0.047}$
P_a	$0.249^{+0.160}_{-0.180}$
β	$-3.87^{+1.77}_{-1.66}$
χ^2_{min}	14.4053

for $P_b \geq 0$, there is a fixed point $\{\Omega_{\rm de} = 1, E = P_b^{1/2}\}$ in the dark energy dominant period. Perform the perturbation expansion of the system near the fixed point and we get the Jacobian matrix

$$M \equiv \begin{pmatrix} \frac{\partial \Omega'_{\rm de}}{\Omega_{\rm de}} & \frac{\partial \Omega'_{\rm de}}{\partial E} \\ \frac{\partial E'}{\partial \Omega_{\rm de}} & \frac{\partial E'}{\partial E} \end{pmatrix} = \begin{pmatrix} -3 & 0 \\ \frac{\beta+3}{2} P_b^{1/2} & \beta \end{pmatrix}. \tag{13}$$

Its eigenvalues are $\lambda_1 = -3$ and $\lambda_2 = \beta$. The stability of the system depends on the sign of the eigenvalues λ_1 and λ_2. For the GP parameterization, β is a real number and not equal to zero, so there are two situations: When $\beta < 0$, the point $\{1, P_b^{1/2}\}$ is an attractor, and when $\beta > 0$, the point $\{1, P_b^{1/2}\}$ is a saddle point. Meanwhile, for $P_b < 0$, we can determine the properties of the fixed point by observing its figure. On the other side, for the case of ΛCDM, the parameter $P_a = 0$, so $\beta\Omega_{\rm de} - \frac{P_b\beta}{E^2} = \beta\frac{P_a a^\beta}{E^2} = 0$, the dynamic system goes to

$$\Omega'_{\rm de} = 3\Omega_{\rm de}(1 - \Omega_{\rm de}), \tag{14}$$

$$E' = -\frac{3}{2}E(1 - \Omega_{\rm de}). \tag{15}$$

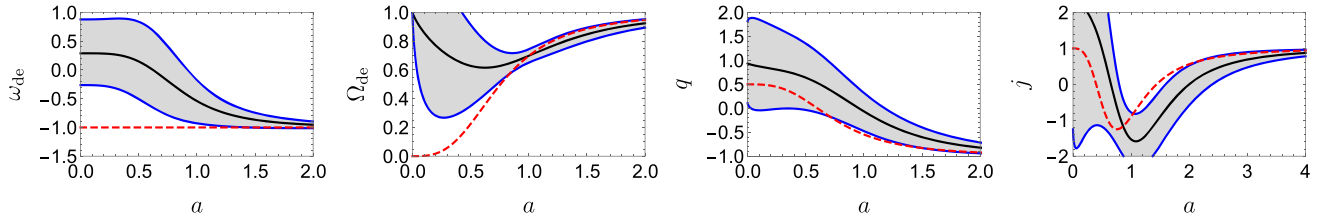

Fig. 2 The evolutions of $\omega_{de}, \Omega_{de}, q$ and j. In each panel, The black line and red dashed line correspond to the GP parameterization and the ΛCDM model, respectively, with the best-fit values listed in Table 3. The shaded region and blue lines represent the 1σ level regions and corresponding boundaries in the GP parameterization

Figure 3a–f illustrate the evolution of the dynamics system for $\beta = -1, 1$ and $P_b = -1, 0, 1$; Fig. 3g shows the situation of $\beta = -3.87$ and $P_b = 0.45$, the red line displays the evolution under the best-fit values listed in Table 3 and the red dot is the current location; Fig. 3h exhibits the evolutional trajectories of the ΛCDM model as a comparison. From Fig. 3a, d, it can be found that there is a saddle point $\{1, 0\}$ for $P_b < 0$. When $\beta > 0$ and $P_b < 0$, it shows that $E \to \infty$ and $\Omega_{de} \to 1$, which is the case of phantom. While for $\beta < 0$ and $P_b < 0$, one can see $\Omega_{de} \to 0$ which corresponds to quintessence. When $P_b \geq 0$, whether the universe is biased towards quintessence or phantom depends on β and initial conditions which cannot be judged directly. According to Fig. 3g, our universe has an attractor $(1, 0.67)$ and H is decreasing. Based on the above analysis, we summarize the stability of the GP parameterization in Table 4.

5 Fate of the universe under the phantom field

In recent years, various data have shown that the dark energy state equation is close to 1: the WMAP9 have found $\omega = -1.073^{+0.090}_{-0.089}$ based on WMAP+CMB+BAO+H_0 [4]. Planck-2018 constrained the EoS as $\omega = -1.03 \pm 0.03$ with SNe [11]. Moreover, DES suggests $\omega = -0.978 \pm 0.059$ in the joint analysis of DES-SN3YR+CMB [57]. Using existing data, it is still impossible to distinguish between phantom ($\omega < -1$) and non-phantom($\omega \geq -1$), that is, the phantom case cannot be excluded. The phantom has gradually increased energy density, and eventually the universe accelerates so fast that the particles lose contact with each other and rip apart. Based on the various evolutionary behaviors of $H(t)$, the final fate of the universe can be divided into the following three categories [58]:

1. Big rip: $H(t) \to \infty$ as $t \to$ constant, so the rip will happen at a certain time.
2. Little rip: $H(t) \to \infty$ as $t \to \infty$. This situation has no singularities in the future.
3. Pseudo-rip: $H(t) \to$ constant. This is the case with the de Sitter universe and little rip.

In this section, we are interested in the rip case of our GP parameterization. For the GP parameterization, the Hubble constant is written as

$$H = \frac{\dot{a}}{a} = H_0(\Omega_{m0}a^{-3} + P_a a^{\beta} + 1 - P_a - \Omega_{m0})^{1/2}. \tag{16}$$

In Sect. 2, we have pointed out that $\beta P_a > 0$ for phantom case of the GP parameterization. Next we discuss each situation separately.

1. $\beta < 0$, $P_a < 0$:

With the growth of cosmic time, $a \to \infty$ and

$$H \to H_0(1 - P_a - \Omega_{m0})^{1/2}, \tag{17}$$

i.e. $H(t)$ tends to be a constant, and the universe will approach the de Sitter universe infinitely. So this case is a pseudo-rip.

2. $\beta > 0$, $P_a > 0$:

When $a \to \infty$,

$$H \to H_0(P_a a^{\beta})^{1/2}. \tag{18}$$

By solving the above differential equation, we can get the relation between the scale factor a and time t, which can be written as

$$a = \left(1 - \frac{\beta P_a^{1/2} H_0}{2}(t - t_0)\right)^{-2/\beta}, \tag{19}$$

where t_0 is the present value of time. Substituting Eq. (19) for Eq. (18), one obtains

$$H = \frac{H_0 P_a^{1/2}}{1 - \frac{\beta P_a^{1/2} H_0}{2}(t - t_0)}. \tag{20}$$

So when $t \to \frac{2}{\beta P_a^{1/2} H_0} + t_0$, $H(t) \to \infty$ which means the universe will have a big rip after $t - t_0 = \frac{2}{\beta P_a^{1/2} H_0}$. Thus, the lifetime of the universe is determined by two parameters, β and P_a, regardless of the matter density Ω_{m0}. Let us make a rough estimate. Take $\beta = 1$, $P_a = 0.02$, $H_0 = 70$ km s^{-1}

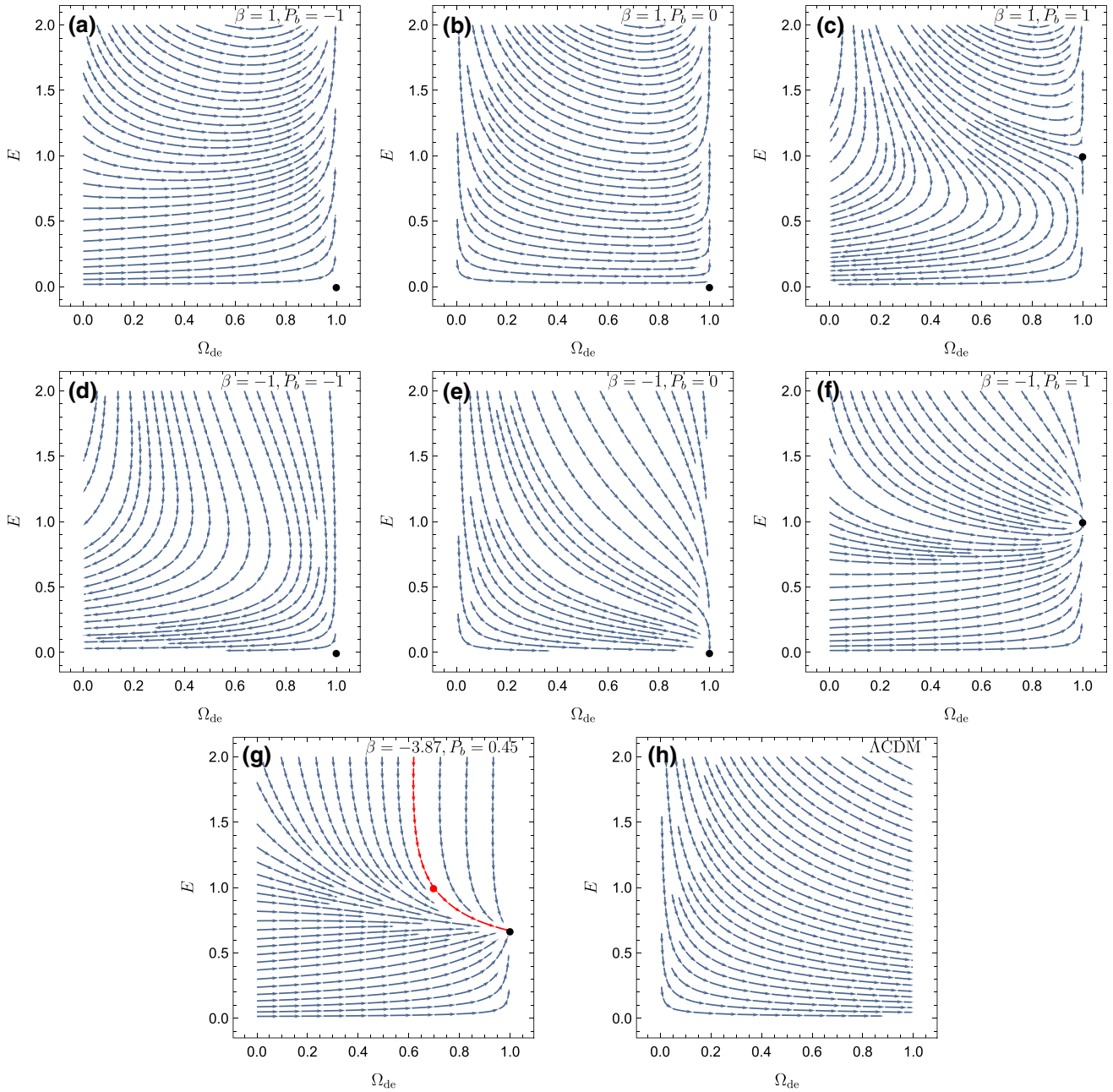

Fig. 3 The dynamic system evolution of the GP parameterization. **a–f** The evolution of the dynamics system for $\beta = -1$, 1 and $P_b = -1$, 0, 1. **g** The situation of $\beta = -3.87$ and $P_b = 0.45$, the red line displays the evolution under the best-fit values listed in Table 3 and the red dot is the current location. For comparison, we also exhibit the scenario of the ΛCDM model in **h**. The arrows stand for the direction of time. The black dots represent the fixed point

Mpc^{-1}, then the universe will be torn apart after 198 Gyr. If 13.8 Gyr is the current age of the universe, then the universe has spent only 6.5% of its life.

3. $\beta \to 0$:

In this case, the GP parameterization degenerates into the model in [45]. According to the discussion in [45], the ultimate fate of the universe is the little rip.

To sum up, there are three possible fates under the phantom of the GP parameterization:

1. Big rip for $\beta > 0$, $P_a > 0$.
2. Little rip for $\beta \to 0$.
3. Pseudo-rip for $\beta < 0$, $P_a < 0$.

Table 4 The stability of the GP parameterization

	$\{\Omega_{de}, E\}$	Stability
$P_b \geq 0, \beta < 0$	$\{1, P_b^{1/2}\}$	Attractor
$P_b \geq 0, \beta > 0$	$\{1, P_b^{1/2}\}$	Saddle point
$P_b < 0$	$\{1, 0\}$	Saddle point

6 Conclusions

In principle, it is interesting to insert models or theories into a more general framework to test their validity. Not only does this reveal a new set of solutions, but it may also enable more accurate consistency checks for the original model. This paper has made this attempt by expanding the ΛCDM model to a generalized pressure (GP) parameterization. The GP parameterization has three independent parameters: The present value of the matter density parameter Ω_{m0}, the parameter P_a, which represents the deviation from the ΛCDM model, and the parameter β. Picking different values of the parameter β can produce three common pressure parametric models. By using the cosmic chronometer (CC) datasets to constrain the parameters, it shows that the Hubble constant is $H_0 = (72.30^{+1.26}_{-1.37})$ km s^{-1} Mpc^{-1}. The differences of H_0 between our results and SHoES [14] and Planck base-ΛCDM [11] are 0.9 σ and 3.5 σ, respectively. In addition, for the GP parameterization, the matter density parameter is $\Omega_{m0} = 0.302^{+0.046}_{-0.047}$, and the universe shows bias towards quintessence. Then we explore the fixed point of this model and find that there is an attractor or a saddle point corresponding to the different values of the parameters. Next, we analyze the rip of the universe in the phantom case and draw the conclusion that there are three possible endings of the universe: Pseudo-rip for $\beta < 0$, $P_a < 0$, big rip for $\beta > 0$, $P_a > 0$ and little rip for $\beta \to 0$. Finally, we estimate that, for the big rip case, the universe has a life span of 198 Gyr.

Dark energy has been proposed for 20 years, but its nature remains unknown. With this parametric model, we can probe the possible deviation further between the dynamic case and the cosmological constant condition through existing data.

Acknowledgements Jun-Chao Wang thanks Wei Zhang for helpful discussions and code guidance about MCMC.

Data Availability Statement This manuscript has no associated data or the data will not be deposited. [Authors' comment: We use public data, so these data can be made public.]

Funded by SCOAP[3].

References

1. A.G. Riess, A.V. Filippenko, P. Challis, A. Clocchiatti, A. Diercks, P.M. Garnavich, R.L. Gilliland, C.J. Hogan, S. Jha, R.P. Kirshner et al., Astron. J. **116**, 1009 (1998)
2. S. Perlmutter, M.S. Turner, M. White, Phys. Rev. Lett. **83**, 670 (1999)
3. D.J. Eisenstein, I. Zehavi, D.W. Hogg, R. Scoccimarro, M.R. Blanton, R.C. Nichol, R. Scranton, H.-J. Seo, M. Tegmark, Z. Zheng et al., Astrophys. J. **633**, 560 (2005)
4. C.L. Bennett, D. Larson, J. Weiland, N. Jarosik, G. Hinshaw, N. Odegard, K. Smith, R. Hill, B. Gold, M. Halpern et al., Astrophys. J. Suppl. Ser. **208**, 20 (2013)
5. P.A. Ade, N. Aghanim, C. Armitage-Caplan, M. Arnaud, M. Ashdown, F. Atrio-Barandela, J. Aumont, C. Baccigalupi, A.J. Banday, R. Barreiro et al., Astron. Astrophys. **571**, A16 (2014)
6. G. Dvali, G. Gabadadze, M. Porrati, Phys. Lett. B **485**, 208 (2000)
7. S.M. Carroll, V. Duvvuri, M. Trodden, M.S. Turner, Phys. Rev. D **70**, 043528 (2004)
8. S. Nojiri, S.D. Odintsov, Phys. Rev. D **68**, 123512 (2003)
9. C. Brans, R.H. Dicke, Phys. Rev. **124**, 925 (1961)
10. V. Sahni, Y. Shtanov, J. Cosmol. Astropart. Phys. **2003**, 014 (2003)
11. N. Aghanim, Y. Akrami, M. Ashdown, J. Aumont, C. Baccigalupi, M. Ballardini, A. Banday, R. Barreiro, N. Bartolo, S. Basak, et al., arXiv preprint. (2018). arXiv:1807.06209
12. S.M. Carroll, Living Rev. Relativ. **4**, 1 (2001)
13. S. Weinberg, Rev. Mod. Phys. **61**, 1 (1989)
14. A. G. Riess, S. Casertano, W. Yuan, L. M. Macri, D. Scolnic, arXiv preprint. (2019). arXiv:1903.07603
15. R.R. Caldwell, R. Dave, P.J. Steinhardt, Phys. Rev. Lett. **80**, 1582 (1998)
16. A. Kamenshchik, U. Moschella, V. Pasquier, Phys. Lett. B **511**, 265 (2001)
17. L. Amendola, Phys. Rev. D **62**, 043511 (2000)
18. T. Chiba, T. Okabe, M. Yamaguchi, Phys. Rev. D **62**, 023511 (2000)
19. I. Zlatev, L. Wang, P.J. Steinhardt, Phys. Rev. Lett. **82**, 896 (1999)
20. R.R. Caldwell, Phys. Lett. B **545**, 23 (2002)
21. R.R. Caldwell, M. Kamionkowski, N.N. Weinberg, Phys. Rev. Lett. **91**, 071301 (2003)
22. S. Nojiri, S.D. Odintsov, Phys. Lett. B **562**, 147 (2003)
23. C. Armendariz-Picon, V. Mukhanov, P.J. Steinhardt, Phys. Rev. D **63**, 103510 (2001)
24. C. Deffayet, X. Gao, D.A. Steer, G. Zahariade, Phys. Rev. D **84**, 064039 (2011)
25. R.J. Scherrer, Phys. Rev. Lett. **93**, 011301 (2004)
26. Y.-F. Cai, E.N. Saridakis, M.R. Setare, J.-Q. Xia, Phys. Rep. **493**, 1 (2010)
27. Z.-K. Guo, Y.-S. Piao, X. Zhang, Y.-Z. Zhang, Phys. Lett. B **608**, 177 (2005)
28. E. Elizalde, S. Nojiri, S.D. Odintsov, Phys. Rev. D **70**, 043539 (2004)
29. J.S. Bagla, H.K. Jassal, T. Padmanabhan, Phys. Rev. D **67**, 063504 (2003)
30. M. Li, Phys. Lett. B **603**, 1 (2004)
31. H. Wei, R.-G. Cai, Phys. Lett. B **660**, 113 (2008)
32. M.C. Bento, O. Bertolami, A.A. Sen, Phys. Rev. D **66**, 043507 (2002)
33. V. Gorini, A. Kamenshchik, U. Moschella, Phys. Rev. D **67**, 063509 (2003)
34. M. Chevallier, D. Polarski, Int. J. Mod. Phys. D **10**, 213 (2001)
35. E.V. Linder, Phys. Rev. Lett. **90**, 091301 (2003)

36. E.M. Barboza Jr., J.S. Alcaniz, Z.-H. Zhu, R. Silva, Phys. Rev. D **80**, 043521 (2009)
37. C. Cattoën, M. Visser, Class. Quantum Grav. **24**, 5985 (2007)
38. C. Gruber, O. Luongo, Phys. Rev. D **89**, 103506 (2014)
39. U. Alam, V. Sahni, T. Deep Saini, A.A. Starobinsky, Mon. Not. R. Astron. Soc. **354**, 275 (2004)
40. A.A. Sen, Phys. Rev. D **77**, 043508 (2008)
41. S. Kumar, A. Nautiyal, A.A. Sen, Eur. Phys. J. C **73**, 2562 (2013)
42. Q. Zhang, G. Yang, Q. Zou, X. Meng, K. Shen, Eur. Phys. J. C **75**, 300 (2015)
43. G. Yang, D. Wang, X. Meng, arXiv preprint. (2016). arXiv:1602.02552
44. D. Wang, Y.-J. Yan, X.-H. Meng, Eur. Phys. J. C **77**, 263 (2017)
45. J.-C. Wang, X.-H. Meng, Commun. Theor. Phys. **70**, 713 (2018)
46. Ö. Akarsu, T. Dereli, Int. J. Theor. Phys. **51**, 612 (2012)
47. C. Zhang, H. Zhang, S. Yuan, S. Liu, T.-J. Zhang, Y.-C. Sun, Res. Astron. Astrophys. **14**, 1221 (2014)
48. M. Moresco, A. Cimatti, R. Jimenez, L. Pozzetti, G. Zamorani, M. Bolzonella, J. Dunlop, F. Lamareille, M. Mignoli, H. Pearce et al., J. Cosmol. Astropart. Phys. **2012**, 006 (2012)
49. R. Jimenez, L. Verde, T. Treu, D. Stern, Astrophys. J. **593**, 622 (2003)
50. M. Moresco, L. Pozzetti, A. Cimatti, R. Jimenez, C. Maraston, L. Verde, D. Thomas, A. Citro, R. Tojeiro, D. Wilkinson, J. Cosmol. Astropart. Phys. **2016**, 014 (2016)
51. D. stern, R. Jimenez, L. Verde, et al., J. Cosmol. Astropart. Phys. **2010**(02), 008 (2010)
52. J. Simon, L. Verde, R. Jimenez, Phys. Rev. D **71**, 123001 (2005)
53. Y. Wang, G.-B. Zhao, C.-H. Chuang, M. Pellejero-Ibanez, C. Zhao, F.-S. Kitaura, S. Rodriguez-Torres, arXiv preprint. (2017). arXiv:1709.05173
54. M. Moresco, Mon. Not. R. Astron. Soc. Lett. **450**, L16 (2015)
55. D. Foreman-Mackey, D.W. Hogg, D. Lang, J. Goodman, Publ. Astron. Soc. Pac. **125**, 306 (2013)
56. S. Bocquet, F.W. Carter, J. Open Source Softw. (2016). https://doi.org/10.21105/joss.00046
57. T. Abbott, S. Allam, P. Andersen, C. Angus, J. Asorey, A. Avelino, S. Avila, B. Bassett, K. Bechtol, G. Bernstein et al., Astrophys. J. Lett. **872**, L30 (2019)
58. P.H. Frampton, K.J. Ludwick, R.J. Scherrer, Phys. Rev. D **85**, 083001 (2012)